# The dynamic mechanical viscoelastic properties of the temporomandibular joint disc: The role of collagen and elastin fibers from a perspective of polymer dynamics

Journal of the Mechanical Behavior of Biomedical Materials 100 (2019) 103406

Contents lists available at ScienceDirect

Journal of the Mechanical Behavior of Biomedical Materials

journal homepage: www.elsevier.com/locate/jmbbm

# The dynamic mechanical viscoelastic properties of the temporomandibular joint disc: The role of collagen and elastin fibers from a perspective of polymer dynamics

Sepanta Fazaeli[a], Samaneh Ghazanfari[b,c], Fereshteh Mirahmadi[a], Vincent Everts[a], Theodoor Henri Smit[d], Jan Harm Koolstra[a,*]

[a] Department of Oral Cell Biology and Functional Anatomy, Academic Centre for Dentistry Amsterdam, University of Amsterdam and Vrije Universiteit Amsterdam, Amsterdam, the Netherlands
[b] Aachen-Maastricht Institute for Biobased Materials, Faculty of Science and Engineering, Maastricht University, Geleen, the Netherlands
[c] Department of Biohybrid & Medical Textiles (Biotex), RWTH Aachen University, Aachen, Germany
[d] Department of Medical Biology - Academic Medical Center Amsterdam, Amsterdam, the Netherlands

ARTICLE INFO

*Keywords:*
Temporomandibular joint disc
Collagen fiber
Elastin fiber
Dynamic mechanical properties
Enzymatic degradation

ABSTRACT

The temporomandibular joint disc is a structure, characterized as heterogeneous fibrocartilage, and is composed of macromolecular biopolymers. Despite a large body of characterization studies, the contribution of matrix biopolymers on the dynamic viscoelastic behavior of the disc is poorly understood. Given the high permeability and low concentration of glycosaminoglycans in the disc, it has been suggested that poro-elastic behavior can be neglected and that the intrinsic viscoelastic nature of solid matrix plays a dominant role in governing its time-dependent behavior. This study attempts to quantify the contribution of collagen and elastin fibers to the viscoelastic properties of the disc. Using collagenase and elastase, we perturbed the collagen and elastin fibrillar network in porcine temporomandibular joint discs and investigated the changes of dynamic viscoelastic properties in five different regions of the disc. Following both treatments, the storage and loss moduli of these regions were reduced dramatically up to the point that the tissue was no longer mechanically heterogeneous. However, the proportion of changes in storage and loss moduli were different for each treatment, reflected in the decrease and increase of the loss tangent for collagenase and elastase treated discs, respectively. The reduction of storage and loss moduli of the disc correlated with a decrease of biopolymer length. The present study indicates that the compositional and structural changes of collagen and elastin fibers alter the viscoelastic properties of the disc consistent with polymer dynamics.

## 1. Introduction

The temporomandibular joint (TMJ) disc is composed of a highly non-homogeneous and deformable fibrocartilaginous tissue (Fig. 1). It facilitates a smooth articulation of the mandibular condyle against the temporal bone during jaw movements (Tanaka and van Eijden, 2003). Due to its unique biochemical composition and structural arrangement of extracellular matrix proteins, the disc plays a crucial role as a congruent agent, stress absorber and stress distributor in the complex jaw kinematics (Tanaka and Koolstra, 2008). The extracellular matrix of the disc is mainly composed of fibrillar collagen (about 70–80% of the dry weight), enriched with a minor amount of glycosaminoglycans (GAGs; about 0.6–10% of the dry weight) and elastin fibers (about 1–3% of the wet weight) embedded in a pool of interstitial fluid (Fazaeli, Ghazanfari, Mirahmadi, Everts, Smit, Koolstra; O'Dell et al., 1990). Regionally, the extracellular matrix components vary in amount and structure and are intimately intertwined within the highly organized collagenous network, forming a skeletal composite that is highly porous and anisotropic with a low permeability (Allen and Athanasiou, 2006).

Understanding the molecular mechanisms of disc biomechanics is not only important for elucidating the disc function but also to understand a degenerative disease like osteoarthritis (OA). Alteration of the load-bearing nature of cartilage during OA progression has been shown previously (Setton et al., 1993). Therefore, understanding the molecular origins of mechanical properties can provide us with new treatment strategies for degenerative diseases and novel approaches towards

* Corresponding author.
*E-mail addresses:* sepantafaz@gmail.com (S. Fazaeli), samaneh.ghazanfari@maastrichtuniversity.nl (S. Ghazanfari), fereshteh.mirahmadi@gmail.com (F. Mirahmadi), veverts@gmail.com (V. Everts), t.h.smit@amsterdamumc.nl (T.H. Smit), j.koolstra@acta.nl (J.H. Koolstra).

https://doi.org/10.1016/j.jmbbm.2019.103406
Received 3 April 2019; Received in revised form 27 July 2019; Accepted 24 August 2019
Available online 26 August 2019
1751-6161/ 

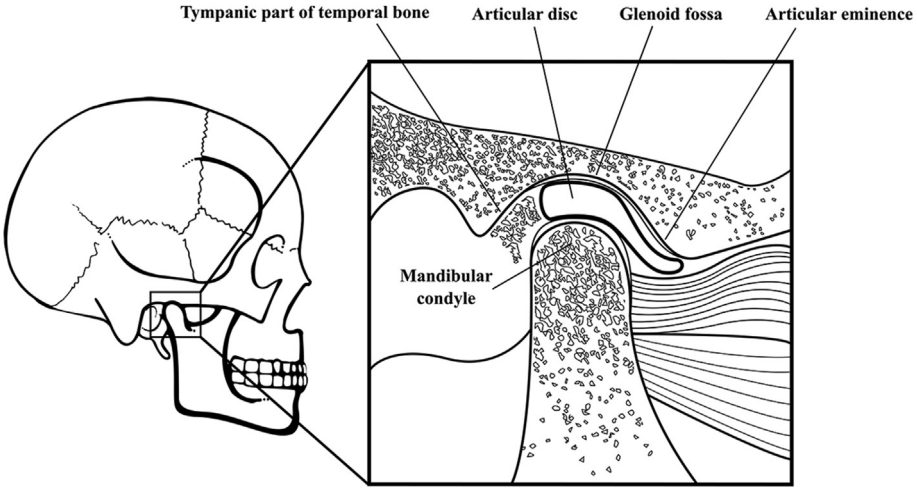


**Fig. 1.** Schematic representation of extracellular matrix (ECM) components of the TMJ disc.

tissue-engineering of the disc. It also helps with developing phenomenological description of tissue behavior which can lead to more accurate predictive and patient-specific computational models.

The behavior of the TMJ disc as a mechanical system is defined by the nature of the applied load and the interaction of the extracellular matrix components (Fazaeli et al., 2016). Under compression, a common form of loading in jaw movement, the disc exhibits viscoelastic behavior, which is dependent on both the amplitude and the rate of deformation (Allen and Athanasiou, 2006). Historically, two mechanisms have been considered responsible for the time-dependent behavior of the cartilage (Huang et al., 2001, 2003; Mow et al., 1980; Stolz et al., 2004 May): (1) a flow-dependent mechanism called poro-elasticity, which implies fluid pressurization and diffusive drag forces generated by fluid flow through and out of the porous matrix, and (2) a flow-independent mechanism, associated with intermolecular friction and intrinsic viscoelastic nature of the solid matrix, exhibited in all polymeric materials.

Many cartilage characterization studies have supported the flow-dependent mechanism by showing that fluid supports as much as 90% of the total stress energy applied on the cartilage under slow quasi-static ($> 100$ s of load application) (Soltz and Ateshian, 1998, 2000; Basalo et al., 2004; Park et al., 2003) or oscillatory ($< 0.01$ Hz) loading conditions (Fortin and Soulhat, 2000). On the other hand, Wong et al. (2000) showed that 70% of the stress in humeral head cartilage relaxed during the first minute of stress-relaxation under unconfined compression without observing any volume change. This indicates that fluid flow is not the only player governing the time-dependent cartilage behavior. While fluid flow and its associated constitutive model (biphasic poro-elasticity) can successfully characterize the long-term mechanics of the cartilage (Mow et al., 1984), they do not accurately describe cartilage behavior at the short term or under higher rates of deformation; more specifically: they fail to capture the fast-oscillatory nature of *in vivo* cartilage loading (0.5–3 Hz) (Huang et al., 2001; Stolz et al., 2004 May; DiSilvestro et al., 2001; Brown and Singerman, 1986; June et al., 2011). This led to the development of biphasic poro-viscoelastic models that not only include the poro-elastic behavior, but also capture the intrinsic viscoelastic nature of the solid matrix under physiological loading conditions (Mak, 1986).

As for the TMJ disc, biphasic and poro-elastic finite element models have considered the fluid pressurization in the matrix as the governing contributor to its time-dependent behavior (Kuo et al., 2010; Spilker et al., 2009; Beek et al., 2003). However, while such models successfully capture the hyaline cartilage mechanical response, they may have limitations regarding the TMJ disc behavior due to the distinguished compositional, structural and mechanical differences between the two. There is a clear difference between the cartilage of the TMJ disc and the cartilage of the articular joints regarding their biphasic mechanical properties: the aggregate modulus of the TMJ disc (100–400 kPa) is approximately three orders of magnitude smaller and its permeability ($5 \times 10^{-15}$ m$^4$/Ns) is about four times higher than of the hyaline cartilage in the knee (Kuo et al., 2010). The higher permeability and sparse scattering of hydrophilic GAGs in the TMJ disc allow fluid to flow throughout the solid matrix with little impedance (i.e. reduced drag between the fluid and solid matrix), leading to a relatively quick relaxation of the disc under stress (5–50 s) (Allen and Athanasiou, 2006). Due to this lower "rate-limiting" effect of fluid pressurization in the TMJ disc, it is thought that the flow-dependent mechanism is even less of a determinant factor in tissue's time-dependent behavior than that of the hyaline cartilage. This view is supported by Setton et al. (1993) who emphasized that the contribution of intrinsic viscoelasticity increases as the permeability of the articular cartilage increases (i.e. surface fibrillation). Given the above considerations, it is thought that the intrinsic viscoelastic nature of the solid matrix plays a dominant role in the TMJ disc time-dependent behavior. This has led others (Allen and Athanasiou, 2006; Koolstra et al., 2007) to suggest that mechanically, the TMJ disc should be modeled as a monophasic viscoelastic solid.

By considering the cartilage as a composite of macromolecular biopolymers (Ferry, 1980; Harper et al., 1984; Fyhrie and Barone, 2003), polymer dynamics has shown to be an apt model to describe its flow-independent viscoelastic behavior (Fyhrie and Barone, 2003; June et al., 2006, 2009; June and Fyhrie, 2009). Polymer dynamics as an approach to characterize cartilage viscoelasticity deepens our understanding of TMJ disc properties and eventually may lead to new therapeutic strategies. Therefore, the present study aims to shed light on the molecular origins of the TMJ disc viscoelastic behavior in the context of polymer dynamics.

In polymer dynamics, the mechanical properties of a material depend on the flexible motions and interactions of high length-to-width entangled polymers (de Gennes, 1971). The theory predicts that stress-relaxation proceeds faster with shorter and more compliant molecules (Doi and Edwards, 1988). This is attributed to the greater microstructure rearrangement due to the increased compliance of the biopolymers, leading to a faster equilibration of the material under the applied deformation. For the oscillatory loading as used in the current study, polymer dynamic predicts that shorter molecular length results in the decrease of dynamic complex modulus, which is reflected in the reduction of both storage and loss modulus (June and Fyhrie, 2009).

Mechano-enzymatic tests have been commonly used to assess the biomechanical contribution of cartilage extracellular matrix molecules (Fazaeli et al., 2016; Stolz et al., 2004 May; June and Fyhrie, 2009;

Greene et al., 2012; Yuan et al., 1985; Griffin et al., 2014 Dec; Willard et al., 2012). In our previous studies (Fazaeli et al., 2016), we characterized the contribution of collagen and elastin fibers under dynamic compressive mechanical loading using collagenase and elastase digestion, respectively. In both studies, following the enzymatic treatment, we observed structural and biochemical changes of the targeted molecules and discussed their associated impact on the instantaneous modulus and maximum hysteresis of the treated discs. In the present study, we aim to quantify the alteration of viscoelastic properties of the TMJ disc following collagenase and elastase digestion. The underlying hypothesis is that the TMJ disc storage and loss moduli will decrease following the enzymatic treatments.

## 2. Materials and methods

### 2.1. Sample preparation

A total of ten young porcine heads (5 heads for each study) were obtained from a local slaughterhouse. The TMJ discs with intact condylar heads were harvested *en bloc*. The discs were then removed from extraneous parts, visually inspected and discarded in case of any gross abnormalities. Next, the discs were washed in phosphate buffered saline (PBS), wrapped in gauze soaked in a solution of PBS and a mixture of protease inhibitors (Roche Diagnostics, Germany). The discs were then stored at −20 °C until used. For further details, see Fazaeli et al. (2016).

### 2.2. Enzymatic digestion

The enzymatic digestion protocol has been described in detail (Fazaeli et al., 2016). Briefly, the left disc of each head was assigned to the control (PBS) group (n = 5) and the right disc to the treated (collagenase or elastase) group (for each treated group n = 5). Solutions of PBS containing collagenase type II (100U/ml, Worthington Inc., Lakewood, NJ) or a mixture of 3U/ml pancreatic elastase (E1250, Sigma, UK) with 0.1 mg/ml soybean trypsin inhibitor (T9003, Sigma, UK) were used for collagenase and elastase digestion, respectively. Samples were treated for 16 h under gentle agitation at 37 °C. All discs were mechanically tested before and after incubation with PBS or the enzymatic solution, thus serving as their own controls.

### 2.3. Testing apparatus and loading conditions

The dynamic viscoelastic properties of the samples were measured with a custom-built material testing machine, which consists of two 4 mm circular flat-ended indenters (stainless-steel) and a chamber. The loading protocol has been described in detail (Fazaeli et al., 2016). Briefly, the desired region of the sample was glued to the bottom indenter using cyanoacrylate (Histoacryl, Braun Surgical S.A., Rubi, Spain), and compressed by the sinusoidal displacement of the top indenter. The displacement was controlled by a custom-made software (implemented in LabVIEW 8.2, National Instruments, Austin, TX), and a 25 N load cell (Honeywell Model 11, Honeywell, Golden Valley, MN) was used to register the normal reaction force applied to the top indenter.

All experiments were performed in the chamber filled with PBS at room temperature. To prevent slippage during the experiment, a tare load of 0.02 N was applied to the sample and the platen-to-platen distance was defined as the thickness of the sample. Then, 20 cycles of dynamic compression with a strain amplitude of 10% and a frequency of 1 Hz were applied to the sample. Following completion of the test at one location, the disc was carefully detached from the bottom indenter and glued at another location for the next test. The same protocol was used to measure the dynamic mechanical properties of control (PBS) and treated (collagenase or elastase) discs at five different regions: posterior band (PB), anterior band (AB), intermediate zone central (IZC), intermediate zone medial (IZM) and intermediate zone lateral (IZL). All regions were loaded in the same order for all samples.

### 2.4. Dynamic viscoelastic parameters

Stress (force divided by cross-sectional area of the indenter) and strain (indenter displacement divided by loaded region thickness) were derived from load-displacement data using routines written in Matlab (MathWorks, Inc., Natick, MA). The viscoelastic behavior of the disc was described using parameters obtained from the stress response to a harmonic (sinusoidal) strain. In the equilibrium state, the stress response of a viscoelastic material also varies sinusoidally but, out of phase with the strain. Thus, the strain (ε) and stress (σ) equations for a viscoelastic material can be written as:

$$\varepsilon = \Delta\varepsilon \sin \omega t \tag{1}$$

and

$$\sigma = \Delta\sigma \sin (\omega t + \delta) \tag{2}$$

Where Δε and Δσ are the amplitudes of strain and stress, respectively. The latter is a function of the angular frequency ω, phase angle tan δ and time *t*. Stress can be rewritten as:

$$\sigma = \Delta\sigma \sin \omega t \cos \delta + \Delta\sigma \cos \omega t \sin \delta \tag{3}$$

which shows that there is one component in phase (Δσ cos δ) and one component out of phase (Δσ sin δ) with the strain. For an elastic material, the stress is in phase with the strain (δ = 0), implying a constant ratio of Δσ/Δε at all times, which represents the Young's modulus *E* (stiffness) of the material. By contrast, if (δ = 1), the stress is 90° out of phase with the strain, representing an absolute viscous material. For a viscoelastic material, the phase angle is between 0° and 90°, which results in a ratio of Δσ/Δε that depends on loading rate or frequency. Thus, the strain amplitude for any frequency allows calculating the phase lag and Δσ/Δε, from which we can further calculate the complex dynamic modulus $E^*$ which consists of a real part, the storage modulus $E'$ and an imaginary part, the loss modulus $E''$ as described below:

$$E^* = E' + iE'' \tag{4}$$

$$\tan \delta = (E'/E'') \tag{5}$$

Where $i = \sqrt{-1}$ and tan δ is the loss tangent. The storage modulus $E'$ represents the elastic nature of the material behavior and is directly proportional to the energy storage in a cycle of deformation. The loss modulus $E''$ exhibits the viscous nature of the material behavior and is proportional to the energy dissipation in a cycle of deformation. The loss tangent (tangent of phase lag) denotes the ratio of dissipated to stored energy during cyclic deformation and is a measure of the materials' tendency to the elastic or viscous behavior. The magnitude of the complex modulus is defined as:

$$|E^*| = (\Delta\sigma/\Delta\varepsilon) \tag{6}$$

where Δσ and Δε are the stress and strain in the equilibrium state. Using the phase lag and the magnitude of complex modulus, the storage and loss moduli are determined as below:

$$E' = |E^*| \cos \delta \tag{7}$$

$$E'' = |E^*| \sin \delta \tag{8}$$

The schematic representation of the described parameters and the stress-strain relationship for an absolute elastic, absolute viscous and a viscoelastic material is shown in Fig. 2. Using the storage modulus ($E'$), the loss modulus ($E''$) and the loss tangent (tan δ) parameters, we will describe the effect of enzymatic treatment (collagenase or elastase) on the viscoelastic behavior of the TMJ disc.

It is important to note that the use of a storage and a loss modulus is defined for small dynamical deformations [-], where the stresses and strains both are perfectly harmonic. In the present study however, we

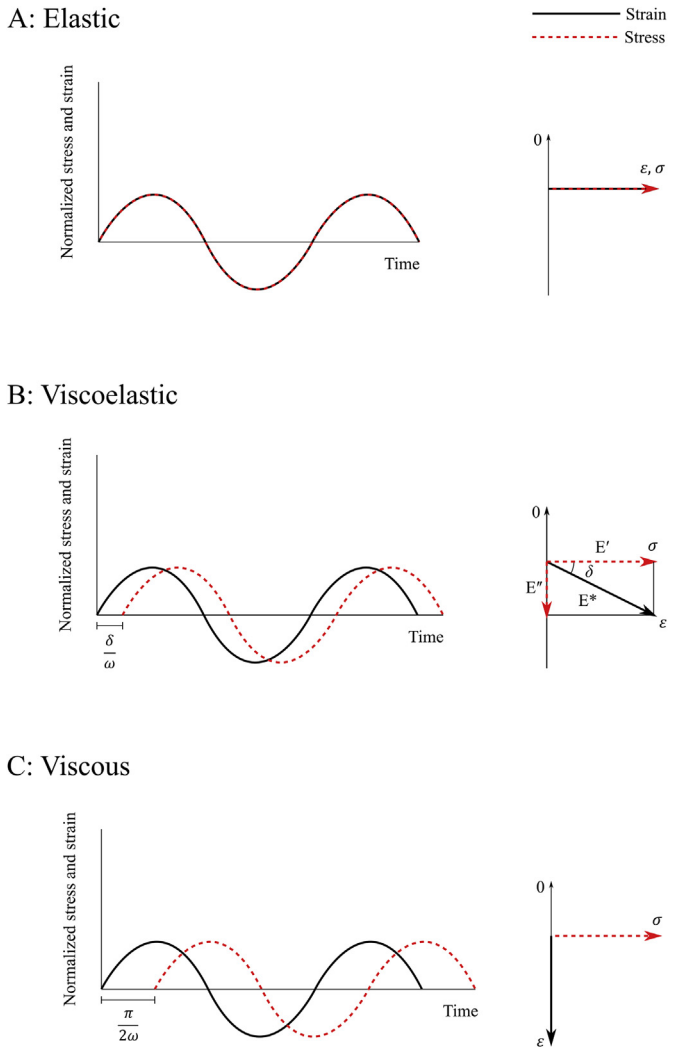


**Fig. 2.** Schematic representation of the relationship between the stress and strain under the application of an oscillatory strain amplitude with an angular velocity of ω. The storage and loss moduli have been represented in the right column for a purely elastic (A), viscoelastic (B) and a perfectly viscous (C) material. In a viscoelastic material, the phase difference (δ) varies between 0° and 90°, resulting in a complex modulus ($E^*$), consisting of a real (storage modulus, $E'$) and an imaginary (loss modulus, $E''$) component, shown in distinguished vectors. The tangent of the phase angle (δ) represents the ratio of energy loss to the energy stored per cycle of loading.

applied a large-strain deformation (10%). Thus, while the stress was closely following the strain path, it dropped faster than complete retreat of the indenter during the unloading phase. Consequently, stress was not perfectly harmonic. Therefore, an approximation of the storage modulus and the loss modulus was derived from the stress-strain curves. Instead of calculating the phase lag based on the moment of maximum strain and stress, the time lag between the moments when the strain and stress curves were halfway their corresponding maximum value was considered.

### 2.5. Statistical analysis

Initially, to eliminate the effect of biological variation on the statistical analysis of the viscoelastic parameters, we performed a paired Student's t-test between the corresponding single regions of the left and right discs. As no significant differences between the viscoelastic parameters of the left and right discs were observed, we continued analyses by considering only the data collected following the PBS incubation or enzymatic (collagenase or elastase) treatment.

Using two-way analysis of variance (ANOVA) with repeated measurements, we compared the overall factors of two independent variables, enzymatic treatment (collagenase or elastase) and disc region (PB, AB, IZM, IZC and IZL) on two dependent variables, storage and loss moduli of the associated groups. A multiple pairwise comparison with Bonferroni's correction was used to investigate the regional differences within each group. The adjusted p-values were used for comparisons. A paired student's t-test determined the differences between the storage and loss moduli within every single region of the control (PBS) and treated (collagenase or elastase) groups. Furthermore, the impact of different treatments (collagenase or elastase) on the loss tangent was investigated by using a paired student's t-test, comparing the values between the treated groups and their associated controls within all individual regions.

Statistical analyses were performed using GraphPad Prism 6.01 (GraphPad Software, La Jolla California) using a significance level of $p < 0.05$.

## 3. Results

### 3.1. Effect of collagenase treatment

The effect of collagenase treatment on storage modulus $E'$ and loss modulus $E''$ of the disc was significant ($p < 0.001$, Figs. 3A–4A, respectively). The two-way ANOVA further revealed an overall significant effect of the disc region on $E''$ ($p < 0.01$) but not on $E'$. Moreover, the multiple pairwise *post hoc* test showed regional variation of $E'$ in the control (PBS) group with IZL being the least and significantly different with the PB and IZM. Similarly, IZL had the lowest $E''$ which was significantly different from PB, IZM and AB. Following the collagenase

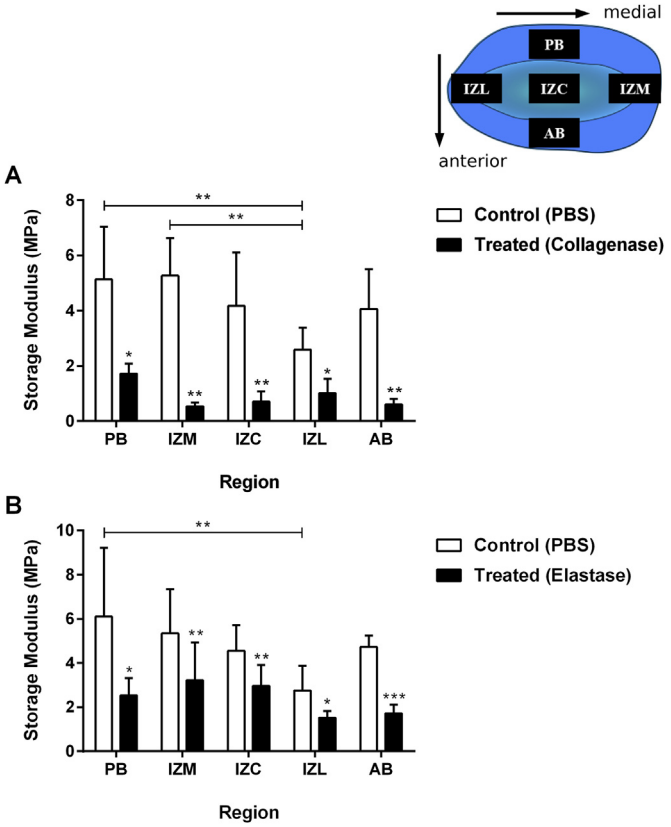


**Fig. 3.** The effect of collagenase (A) and elastase (B) treatment on the storage modulus of the TMJ disc. Data are presented as mean ± SD. * indicates $p < 0.05$, ** indicates $p < 0.01$ and *** indicates $p < 0.001$.

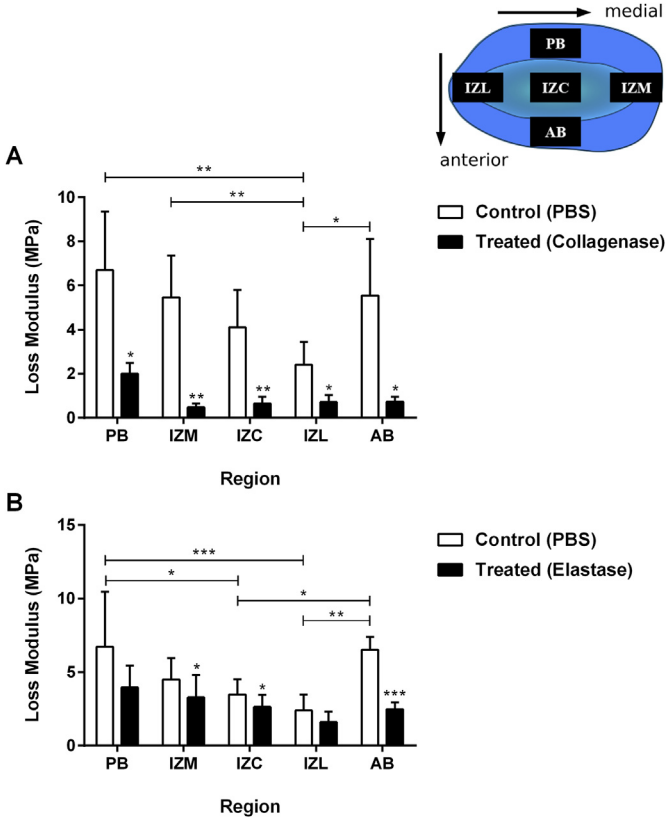


**Fig. 4.** The effect of collagenase (A) and elastase (B) treatment on the loss modulus of the TMJ disc. Data are presented as mean ± SD. * indicates $p < 0.05$, ** indicates $p < 0.01$ and *** indicates $p < 0.001$.

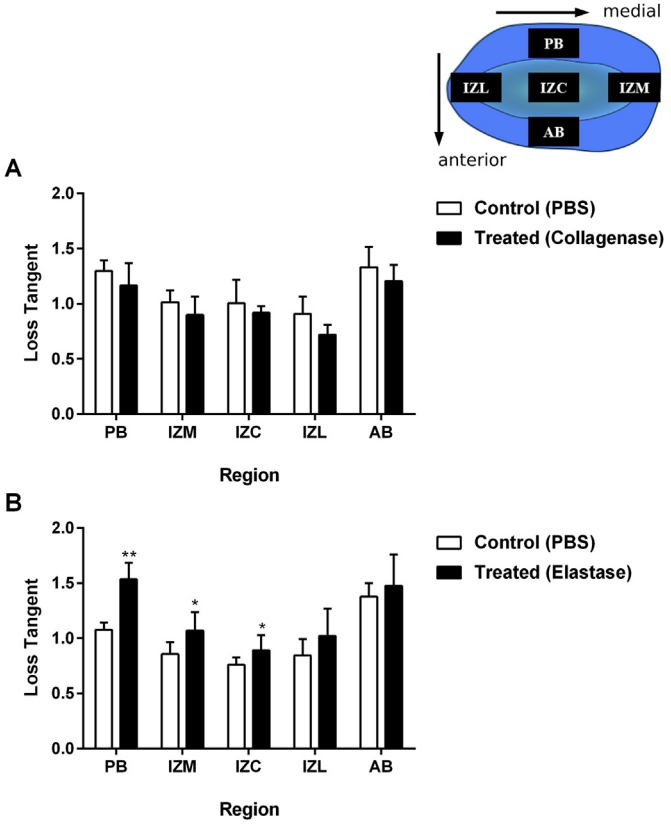


**Fig. 5.** The effect of collagenase (A) and elastase (B) treatment on the loss tangent of the TMJ disc. Data are presented as mean ± SD. * indicates $p < 0.05$, and ** indicates $p < 0.01$.

treatment, the regional variations in $E'$ and $E''$ were no longer present.

According to the paired *t*-test, collagenase treatment dramatically reduced the $E'$ in all regions of the disc (Fig. 3A), where the effect was most significant in the IZM (90%), followed by the AB (85%), IZC (83%), PB (66%) and IZL (61%). A similar pattern was observed for the $E''$ (Fig. 4A) with the IZM undergoing the most significant reduction (91%), followed by the AB (87%), IZC (84%), PB (70%) and IZL (70%).

### 3.2. Effect of elastase treatment

The effect of elastase treatment on $E'$ and $E''$ of the disc was also significant ($P < 0.001$, Figs. 3B–4B, respectively). The two-way ANOVA further revealed an overall significant effect of the disc region on $E$" ($p < 0.01$), but not on the $E$'. The multiple pairwise *post hoc* analysis showed regional variations of $E'$ and $E''$ in the control (PBS) group. IZL had the lowest $E'$ and was significantly different from PB. Moreover, PB had the highest $E''$ and was significantly different from the IZC and IZL. AB had a significantly higher $E''$ than IZC and IZL. Following the elastase treatment, the regional variations were no longer statistically significant for the $E'$ and $E''$.

A paired *t*-test showed a significant reduction of the $E'$ in all regions of the disc following the elastase treatment (Fig. 3B). More specifically, the AB was impacted the most (64%), followed by the PB (41%), IZL (45%), IZM (40%) and IZC (35%). Similarly, the elastase treatment decreased the $E''$ in all regions of the disc (Fig. 4B) with the significant effect, being the most in the AB (62%), followed by the IZM (27%) and IZC (25%).

The effect of treatments on the tan δ is shown in Fig. 5. The collagenase treatment seemed to decrease tan δ in all regions, although the effect was not significant (Fig. 5A). By contrast, the elastase treatment resulted in a noticeable increase of the tan δ in all regions of the disc (Fig. 5B), indicating an increased tendency of damping. However, this increase was only significant in the PB (42%), IZM (25%) and IZC (21%).

## 4. Discussion

The present study has been performed to characterize the molecular origins of viscoelastic properties in the TMJ disc under dynamic compression. We assessed dynamic viscoelastic properties of the TMJ disc before and after enzymatic treatment with collagenase or elastase as performed, analyzed and verified with polarized light microscopy, confocal microscopy and transmission electron microscopy in previous studies (Fazaeli et al., 2016). We measured force and displacement in time and approximated storage modulus, loss modulus and loss tangent as three parameters describing the viscoelastic behavior of the TMJ disc before and after enzymatic treatment. As hypothesized, both treatments dramatically reduced both storage and loss moduli of the disc, the collagenase more strongly than the elastase. The collagenase treated samples got a lower damping ratio of the material, while the elastase treated group showed an increase in damping ratio. We attribute this finding to the decrease in average biopolymer molecular length and entanglement. Polymer dynamic assumes that the cartilage contains numerous long-chain biopolymers that are highly entangled and non-dilute, governing the mechanical behavior of the cartilage via interaction between neighboring biopolymers (Doi and Edwards, 1988). Following the so-called “reptation” model, each polymer chain is at any instant constrained within a ‘tube’ constructed of the adjacent polymer chains, so that they cannot intersect each other (de Gennes, 1971). Thus, the polymer chains move in their tubes like a snake (Ferry, 1980; Doi and Edwards, 1988). Once the polymer system is under loading, the polymer chains can escape from the constraining tubes by reptation, leaving the chains remaining in their original tube responsible for load-bearing (Fyhrie and Barone, 2003). Our results are consistent with these

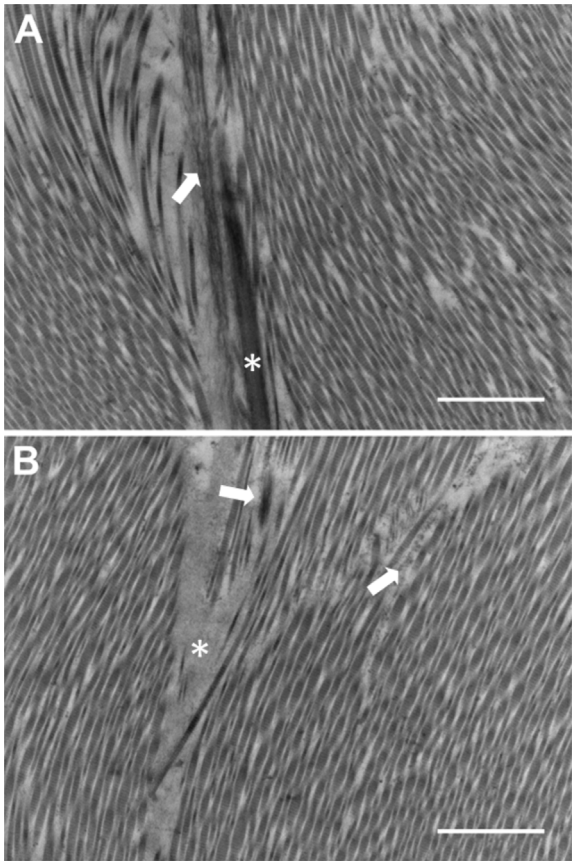


**Fig. 6.** Transmission electron micrographs of intermediate zone central of porcine TMJ disc before (A) and after (B) elastase treatment. (A) Two different stages of elastin fiber development are visible: (1) a premature elastin fiber (white arrowhead) is seen as microfibrils, assembling together to create a layout where elastin will be deposited. (2) a mature elastin fiber (white asterisk) can be recognized by its amorphous elastin core and surrounding microfibrils. These fibers seem to be running along the collagen fibrils, which are distinguishable by their distinctive D-periodic banding pattern. (B) After elastase treatment, hardly any elastin fibers could be spotted, except some elastin devoid areas in the middle of collagen fibrils (white asterisk), seemingly containing some remnants of microfibrils (white arrowhead) and elastin. Except the appearance of these void spaces, the collagen fibrils arrangement did not seem to be affected by the elastase treatment. Scale bar: 2 μm.

interpretive models, suggesting that dynamic mechanical properties of the TMJ disc are sensitive to the matrix composition as well as biopolymer length, interconnectivity and entanglement of the fibrous matrix.

Previously, we observed the disruption of elastin fibers in confocal images and a reduction of matrix compositions biochemically, following elastase treatment (Fazaeli, Ghazanfari, Mirahmadi, Everts, Smit, Koolstra). With interfibrillar components being removed following the elastase treatment, the interfibrillar voids increase, thereby enhancing the rearrangement of the less-constrained collagen fibers (Weisbecker et al., 2013; Schriefl et al., 2015 Apr; Lee et al., 2001; Smith et al., 2008 Feb). In our previous study (Fazaeli, Ghazanfari, Mirahmadi, Everts, Smit, Koolstra), we indeed observed empty interfibrillar spaces, using transmission electron microscopy. These spaces were likely indicative for the presence of elastin fibers residing there before the treatment (Fig. 6, (Fazaeli, Ghazanfari, Mirahmadi, Everts, Smit, Koolstra)). Disruption of the elastin network also compromises the recoiling ability and the resting shape of the tissue upon load removal, leaving the collagen fibers in a less confined and wavy state, thereby affecting the load-bearing capacity of the TMJ disc (Fazaeli, Ghazanfari, Mirahmadi, Everts, Smit, Koolstra). This particular effect of elastase digestion has been discussed previously for other tissues (Schriefl et al., 2015 Apr; Lee et al., 2001; Yapp and Chen, 2015; Chow et al., 2013) and is also reflected in a substantial reduction of collagen tortuosity and a noticeable volume enlargement of the treated discs in our earlier study (Fazaeli, Ghazanfari, Mirahmadi, Everts, Smit, Koolstra). Based on these observations, we speculate that removal of elastin fibers reduced the recoiling ability of the disc, thus accelerating the disc reaching its relaxed state. Also, disruption of the elastin fibers along with loss of interfibrillar medium disanchored the collagen fibers from the matrix, which effectively enhanced the “reptation” effect and consequently left less biopolymers in place to withstand the applied load. Therefore, the elastase treatment reduced both storage and loss moduli of the TMJ disc by perturbing the biopolymer microstructure of the extracellular matrix. This is in agreement with Yuan et al. (1985) and Ventre et al. (2009) who reported reduction of both moduli in elastase treated lung strips under sinusoidal stretch and dermis under sinusoidal shear, respectively.

Regarding the collagenase treatment, a dramatic reduction of storage and loss moduli in the treated discs was observed. In conjunction with our finding, June et al. (June and Fyhrie, 2009) observed a notable reduction of both moduli following collagenase treatment of bovine calf cartilage samples under dynamic compression. Similar observations were reported for collagenase treated cartilage (Hayes and Bodine, 1978) and lung strips (Yuan et al., 1985) under sinusoidal shear and stretch loading, respectively. This dramatic effect of collagenase digestion on the storage and loss moduli is consistent with interpretive network-based models developed for cross-linked biopolymers. In these models, a biopolymer material is modeled as a disordered network of fibers, consisting of densely-connected rigid regions and sparsely connected flexible regions. Based on these models, the fibrous network becomes mechanically rigid only above the so called “rigidity percolation threshold” (Zernia and Huster, 2006). More specifically, the stiffness of the system is strongly dependent on the connectivity of the fibers near the rigidity percolation threshold, above which the fibers are sufficiently connected so that they can transmit the stress from one fibril to another via either interconnectivity or proteoglycan mediated links. Below the threshold, the network is too fragmented to accommodate the external strain, which results in a sharp reduction of the modulus (Griffin et al., 2014 Dec). In another study, using polarized light microscopy, we observed extreme loss of structural integrity and haphazard arrangement of the collagenous network of the disc following collagenase treatment (Fazaeli et al., 2016). Therefore, the effect of collagenase digestion can be considered as an enzymatically driven transition, perturbing the entanglement of the collagenous network and thus, the structural integrity of the matrix in the disc, which results in dramatic reduction of the storage and loss moduli. This observation has been previously explored in detail for shear properties of articular cartilage (Griffin et al., 2014 Dec). More specifically, Silver et al. (2000) have associated the elasticity and viscosity of tendons to the extent of type I collagen crosslinking and collagen fibril length, respectively. They further studied the viscoelastic behavior of osteoarthritic human cartilage and reported a decrease of its elasticity and viscosity with increased fibrillation and fissure formation, attributed to a combination of decreased collagen fibril length, disruption of the interfibrillar crosslinking and loss of the superficial layer (Silver et al., 2001).

While collagenase and elastase both decreased the storage and loss moduli of the discs, the extent and pattern of these effects were quite different. The collagenase treatment reduced the storage and loss moduli across the disc by an average of 77% and 81%, respectively, while the corresponding values for the elastase treatment were only 48% and 38%. These differences were clearly reflected in the corresponding loss tangent values of the treated discs with the collagenase treatment producing an average reduction of 12% and elastase treatment resulting in an average increase by 23%. Our data is in agreement with Yuan et al. (1985) and Ventre et al. (2009) who also reported changes in loss tangent following the collagenase or elastase treatment

of their samples. However, they did not find a significant variation of the loss tangent due to a proportional decrease of storage and loss modulus in their studies. While we observed a proportional reduction of the moduli following a collagenase treatment, elastase digestion changed the loss tangent in favor of viscosity, with less reduction of loss modulus compared to the storage modulus. This was expected as we observed a distinctive effect of elastase and collagenase treatment on the structure, composition and mechanical properties of the TMJ disc in our previous studies (Fazaeli et al., 2016). The collagenase treatment harshly perturbed the structural integrity of the collagenous network and compromised the mechanical properties of the system as whole (Fazaeli et al., 2016). The effect of elastase was more complex as it disrupted the mechanical coupling between elastin and collagen fibers through disengaging the intimate connection between the two networks, resulting in a less confined uncrimping and rearrangement of collagen fibers during the loading (Fazaeli, Ghazanfari, Mirahmadi, Everts, Smit, Koolstra).

Although loading regimens are different, the dynamic moduli are comparable with the relaxed moduli in stress-relaxation test (Tanaka et al., 2014; Chin et al., 1996). Likewise, the dynamic moduli of our control (PBS) group is consistent with Tanaka et al. (2006), who reported a relaxed compressive modulus of bovine TMJ disc samples with a similar strain rate and amplitude as ours. Our data is also in agreement with Tanaka et al. (2003) who reported steady modulus for porcine samples under dynamic compression test, using the same loading settings. Meanwhile, our dynamic moduli are approximately 100 times larger than the ones reported by Fernández et al. (2013), who used porcine samples but a significantly smaller strain amplitude. The 1% strain amplitude used in their study represents the disc's behavior merely in the toe region of the stress-strain curve where collagen fibers are not fully engaged and still are in their wavy state (Berkovitz, 2000a, 2000b). This remarkable difference supports the strain-dependency of the cartilage mechanical properties that has been commonly discussed previously (Allen and Athanasiou, 2005, 2006). Regarding regional variations, the disc exhibits a heterogeneous nature for both storage and loss moduli. In line with (Allen and Athanasiou, 2006), we found the PB and IZM to be stiffer than other regions by showing higher storage modulus. Also, similar to Willard et al. (2012), our data shows that the PB and AB are more viscous than the intermediate regions by showing higher loss modulus. This heterogeneous viscoelastic property of the TMJ disc could provide insight into the functional role of the disc within the complex jaw kinematics. Given the resting position of the disc, articulation would start by rotation of the condylar bone and resistance of relatively stiff and viscous PB against the applied compression, which will promote the rotation of the condylar head towards the less stiff and less viscous IZC (Allen and Athanasiou, 2006). Therefore, deviation from the articulation path towards the less stiff and less viscous regions (e.g. IZL), could potentially cause an unfavorable loading pattern, leading to overloading of the disc. This could result in a hypoxic-reperfusion cycle, initiating a degenerative process (Nitzan, 2001; Mapp et al., 1995). Consequently, overloading could degrade the disc up to a point that perforation appears at the overloaded regions. This explanation is supported by finite element simulation of bruxism (Commisso et al., 2014) and also common observation of perforations in the lateral region of the disc (Werner et al., 1991).

The relative difference between stiffness and viscosity in different regions facilitate the disc to conform its shape, distribute the stress and dissipate the excessive strain energy during the jaw movement (Tanaka and van Eijden, 2003). Structural and compositional changes of elastin and collagen fibers can occur naturally through aging or pathologically as in degenerative conditions, potentially leading to irreversible mechanical changes in the tissue (Fonck et al., 2007). Any triggering factor that disturbs the balance between the activated degenerative proteases and the functional inhibitory system of the ECM can initiate or exacerbate a self-reinforcing degenerative process, referred as the “vicious circle” by Vergroesen et al. (2015) (see Fig. 2 therein). The synovial fluid of the diarthrodial joints with rheumatoid arthritis have been reported to contain higher level of degenerative enzymes such as elastase (Virca et al., 1984; Huet et al., 1992a). Exposure of TMJ components to the synovial fluid containing proteases can also provoke structural and compositional changes in the ECM. Our results suggest that the collagenase and elastase digestions reduce the resiliency and energy dissipation capability of the disc, resulting in a mechanically weakened disc that can no longer act as a shock absorber and is prone to further damage and fracture. This is of clinical importance as the disc in patients with internal derangement has shown to be more rigid and less capable of energy dissipation (Tanaka et al., 2000). Also, in a study by Mow and Lai (1979), they reported decrease of storage and loss moduli in cartilage with increase of age and progression of osteoarthritis. Given the higher level of elastase and collagenase proteases expression in synovial fluid of pathological diarthrodial joints (Srinivas et al., 2001; Jones et al., 2008; Huet et al., 1992b), our data suggest that any extrinsic or intrinsic factor that perturb the collagen or elastin fibrillar network could result in a chemically and structurally different tissue that can reduce the resiliency and viscosity of different regions up to the point that the tissue loses its characteristic heterogeneity and viscoelastic properties. This will compromise the stress distribution and energy dissipation capabilities of the disc, which could lead to an adverse loading condition; thereby initiating or exacerbating an existing degenerative process in the disc (Vergroesen et al., 2015; de Bont and Stegenga, 1993).

In the light of presented findings, we suggest that polymer dynamics can be a useful approach for quantitatively characterizing the TMJ disc flow-independent viscoelasticity behavior. Furthermore, a proper understanding of the specific types of polymer motions and molecular length distribution can further benefit us by developing accurate patient-specific computational models, detecting the potential pathological conditions at early stages. Moreover, application of polymer dynamics can provide us with new benchmarks for tissue engineering and developing novel strategies for designing and tailoring scaffolds to better mimic the natural physiochemical properties of the native tissue.

## 5. Limitations

Due to the relatively small sample size used in this study, the findings should be interpreted cautiously in light of the data limitations for these outcomes. The dynamic compressive loading was performed in PBS at room temperature (25 °C) and not in the synovial fluid of TMJ joints at body temperature; therefore, our testing configurations did not mimic the *in vivo* TMJ disc responses to dynamic loading. Those configurations, however, are sufficient to meet our objective of distinguishing the impact of different treatments (collagenase or elastase) on the dynamic viscoelastic properties of the TMJ disc.

## Author contributions

S.F., S.G., F.M., V.E., T.H.S. and J.H.K. designed the experiments; S.F. and S.G. and F.M. conducted the experiments; S.F. analyzed the data and wrote the manuscript text. All authors reviewed the manuscript.

## Conflicts of interest

The authors have declared that no conflict of interest exists.

## Acknowledgment

The authors would like to thank Sara Ghazanfari for her great help in data analyses.

## Appendix A. Supplementary data

Supplementary data to this article can be found online at https://doi.org/10.1016/j.jmbbm.2019.103406.

## References


Allen, K.D., Athanasiou, K.A., 2005 Jul. A surface–regional and freeze–thaw characterization of the porcine temporomandibular joint disc. Ann. Biomed. Eng. 33 (7), 951–962.

Allen, K.D., Athanasiou, K.A., 2006. Viscoelastic characterization of the porcine temporomandibular joint disc under unconfined compression. J. Biomech. 39 (2), 312–322.

Basalo, I.M., Mauck, R.L., Kelly, T.-A.N., et al., 2004 Dec. Cartilage interstitial fluid load support in unconfined compression following enzymatic digestion. J. Biomech. Eng. 126 (6), 779–786.

Beek, M., Koolstra, J.H., van Eijden, T.M.G.J., 2003 Jan. Human temporomandibular joint disc cartilage as a poroelastic material. Clin. Biomech. 18 (1), 69–76.

Berkovitz, B.K., 2000 Sepa. Collagen crimping in the intra-articular disc and articular surfaces of the human temporomandibular joint. Arch. Oral Biol. 45 (9), 749–756.

Berkovitz, B.K., 2000 Julb. Crimping of collagen in the intra-articular disc of the temporomandibular joint: a comparative study. J. Oral Rehabil. 27 (7), 608–613.

Brown, T.D., Singerman, R.J., 1986. Experimental determination of the linear biphasic constitutive coefficients of human fetal proximal femoral chondroepiphysis. J. Biomech. 19 (8), 597–605.

Chin, L.P., Aker, F.D., Zarrinnia, K., 1996 Mar. The viscoelastic properties of the human temporomandibular joint disc. J. Oral Maxillofac. Surg. 54 (3), 315–319.

Chow, M.-J., Mondonedo, J.R., Johnson, V.M., Zhang, Y., 2013 Apr. Progressive structural and biomechanical changes in elastin degraded aorta. Biomechanics Model. Mechanobiol. 12 (2), 361–372.

Commisso, M.S., Martínez-Reina, J., Mayo, J., 2014 Jun. A study of the temporomandibular joint during bruxism. Int. J. Oral Sci. 6 (2), 116–123.

de Bont, L.G., Stegenga, B., 1993 Apr. Pathology of temporomandibular joint internal derangement and osteoarthrosis. Int. J. Oral Maxillofac. Surg. 22 (2), 71–74.

de Gennes, P.G., 1971. Reptation of a polymer chain in the presence of fixed obstacles. J. Chem. Phys. 55 (2), 572–579.

DiSilvestro, M.R., Zhu, Q., Wong, M., Jurvelin, J.S., Suh, J.K., 2001 Apr. Biphasic poroviscoelastic simulation of the unconfined compression of articular cartilage: I–Simultaneous prediction of reaction force and lateral displacement. J. Biomech. Eng. 123 (2), 191–197.

Doi, M., Edwards, S.F., 1988. The Theory of Polymer Dynamics. Oxford University Press.

Fazaeli, S., Ghazanfari, S., Everts, V., Smit, T.H., Koolstra, J.H., 2016 Jul. The contribution of collagen fibers to the mechanical compressive properties of the temporomandibular joint disc. Osteoarthr. Cartil. 24 (7), 1292–1301.

Fazaeli S, Ghazanfari S, Mirahmadi F, Everts V, Smit TH, Koolstra JH. Effects of Elastase on the Structural and Mechanical Properties of the Temporomandibular Joint Disc. (Submitted for publication).

Fernández, P., Lamela, M.J., Ramos, A., Fernández-Canteli, A., Tanaka, E., 2013 Feb 22. The region-dependent dynamic properties of porcine temporomandibular joint disc under unconfined compression. J. Biomech. 46 (4), 845–848.

Ferry, J.D., 1980. Viscoelastic Properties of Polymers. John Wiley & Sons.

Fonck, E., Prod'hom, G., Roy, S., et al., 2007 Jun. Effect of elastin degradation on carotid wall mechanics as assessed by a constituent based biomechanical model. Am. J. Physiol. Heart Circ. Physiol. 292 (6), H2754–H2763.

Fortin, M., Soulhat, J., 2000 Apr. Unconfined compression of articular cartilage: nonlinear behavior and comparison with a fibril-reinforced biphasic model. J. Biomech. Eng. 122 (2), 189–195.

Fyhrie, D.P., Barone, J.R., 2003 Oct. Polymer dynamics as a mechanistic model for the flow-independent viscoelasticity of cartilage. J. Biomech. Eng. 125 (5), 578–584.

Greene, G.W., Zappone, B., Banquy, X., et al., 2012. Hyaluronic acid-collagen network interactions during the dynamic compression and recovery of cartilage. Soft Matter 8 (38), 9906–9914.

Griffin, D.J., Vicari, J., Buckley, M.R., Silverberg, J.L., Cohen, I., Bonassar, L.J., 2014 Dec Dec. Effects of enzymatic treatments on the depth-dependent viscoelastic shear properties of articular cartilage. J. Orthop. Res. 32 (12), 1652–1657.

Harper, G.S., Comper, W.D., Preston, B.N., 1984 Aug 25. Dissipative structures in proteoglycan solutions. J. Biol. Chem. 259 (16), 10582–10589.

Hayes, W.C., Bodine, A.J., 1978. Flow-independent viscoelastic properties of articular cartilage matrix. J. Biomech. 11 (8-9), 407–419.

Huang, C.Y., Mow, V.C., Ateshian, G.A., 2001 Oct. The role of flow-independent viscoelasticity in the biphasic tensile and compressive responses of articular cartilage. J. Biomech. Eng. 123 (5), 410–417.

Huang, C.-Y., Soltz, M.A., Kopacz, M., Ateshian, G.A., 2003 Feb. Experimental verification of the roles of intrinsic matrix viscoelasticity and tension-compression nonlinearity in the biphasic response of cartilage. J. Biomech. Eng. 125 (1), 84–93.

Huet, G., Filipo, R.M., Richet, C., et al., 1992 Sepa. Measurement of elastase and cysteine proteinases in synovial fluid of patients with rheumatoid arthritis, sero-negative spondylarthropathies, and osteoarthritis. Clin. Chem. 38 (9), 1694–1697.

Huet, G., Flipo, R.M., Richet, C., Thiebaut, C., 1992 Sepb. Measurement of elastase and cysteine proteinases in synovial fluid of patients with rheumatoid arthritis, sero-negative spondylarthropathies, and osteoarthritis. Clin. Chem. 38 (9), 1694–1697.

Jones, G.C., Riley, G.P., Buttle, D.J., 2008. The role of proteases in pathologies of the synovial joint. Int. J. Biochem. Cell Biol. 40 (6-7), 1199–1218.

June, R.K., Fyhrie, D.P., 2009 Nov 4. Enzymatic digestion of articular cartilage results in viscoelasticity changes that are consistent with polymer dynamics mechanisms. Biomed. Eng. Online 8, 32.

June, R.K., Barone, J.R., Fyhrie, D.P., 2006. Cartilage stress-relaxation described by polymer dynamics. In: Annual Meeting of the Orthopaedic Research Society. Chicago, IL.

June, R.K., Ly, S., Fyhrie, D.P., 2009 Mar 1. Cartilage stress-relaxation proceeds slower at higher compressive strains. Arch. Biochem. Biophys. 483 (1), 75–80.

June, R.K., Neu, C.P., Barone, J.R., Fyhrie, D.P., 2011 May 10. Polymer mechanics as a model for short-term and flow-independent cartilage viscoelasticity. Mater Sci Eng C Mater Biol Appl 31 (4), 781–788.

Koolstra, J.H., Tanaka, E., van Eijden, T.M.G.J., 2007. Viscoelastic material model for the temporomandibular joint disc derived from dynamic shear tests or strain-relaxation tests. J. Biomech. 40 (10), 2330–2334.

Kuo, J., Zhang, L., Bacro, T., Yao, H., 2010 May 7. The region-dependent biphasic viscoelastic properties of human temporomandibular joint discs under confined compression. J. Biomech. 43 (7), 1316–1321.

Lee, T.C., Midura, R.J., Hascall, V.C., Vesely, I., 2001 Feb. The effect of elastin damage on the mechanics of the aortic valve. J. Biomech. 34 (2), 203–210.

Mak, A.F., 1986 May. The apparent viscoelastic behavior of articular cartilage—the contributions from the intrinsic matrix viscoelasticity and interstitial fluid flows. J. Biomech. Eng. 108 (2), 123–130.

Mapp, P.I., Grootveld, M.C., Blake, D.R., 1995. Hypoxia, Oxidative Stress and Rheumatoid Arthritis. Europepmcorg.

Mow, V.C., Lai, W.M., 1979. Mechanics of animal joints. Annu. Rev. Fluid Mech. 11 (1), 247–288.

Mow, V.C., Kuei, S.C., Lai, W.M., Armstrong, C.G., 1980 Feb. Biphasic creep and stress relaxation of articular cartilage in compression? Theory and experiments. J. Biomech. Eng. 102 (1), 73–84.

Mow, V.C., Holmes, M.H., Lai, W.M., 1984. Fluid transport and mechanical properties of articular cartilage: a review. J. Biomech. 17 (5), 377–394.

Nitzan, D.W., 2001. The Process of Lubrication Impairment and its Involvement in Temporomandibular Joint Disc Displacement: a Theoretical Concept. Elsevier.

O'Dell, N.L., Starcher, B.C., Wilson, J.T., Pennington, C.B., Jones, G.A., 1990. Morphological and biochemical evidence for elastic fibres in the syrian hamster temporomandibular joint disc. Arch. Oral Biol. 35 (10), 807–811.

Park, S., Krishnan, R., Nicoll, S.B., Ateshian, G.A., 2003 Dec. Cartilage interstitial fluid load support in unconfined compression. J. Biomech. 36 (12), 1785–1796.

Schriefl, A.J., Schmidt, T., Balzani, D., Sommer, G., Holzapfel, G.A., 2015 Apr Apr. Selective enzymatic removal of elastin and collagen from human abdominal aortas: uniaxial mechanical response and constitutive modeling. Acta Biomater. 17, 125–136.

Setton, L.A., Zhu, W., Mow, V.C., 1993 Apr-May. The biphasic poroviscoelastic behavior of articular cartilage: role of the surface zone in governing the compressive behavior. J. Biomech. 26 (4-5), 581–592.

Silver, F.H., Christiansen, D.L., Snowhill, P.B., Chen, Y., 2000. Role of storage on changes in the mechanical properties of tendon and self-assembled collagen fibers. Connect. Tissue Res. 41 (2), 155–164.

Silver, F.H., Bradica, G., Tria, A., 2001. Viscoelastic behavior of osteoarthritic cartilage. Connect. Tissue Res. 42 (3), 223–233.

Smith, L.J., Byers, S., Costi, J.J., Fazzalari, N.L., 2008 Feb Feb. Elastic fibers enhance the mechanical integrity of the human lumbar anulus fibrosus in the radial direction. Elastic fibers enhance the mechanical integrity of the human lumbar anulus fibrosus in the radial direction. Ann. Biomed. Eng. 36 (2), 214–223.

Soltz, M.A., Ateshian, G.A., 1998 Oct. Experimental verification and theoretical prediction of cartilage interstitial fluid pressurization at an impermeable contact interface in confined compression. J. Biomech. 31 (10), 927–934.

Soltz, M.A., Ateshian, G.A., 2000 Feb. Interstitial fluid pressurization during confined compression cyclical loading of articular cartilage. Ann. Biomed. Eng. 28 (2), 150–159.

Spilker, R.L., Nickel, J.C., Iwasaki, L.R., 2009 Jun. A biphasic finite element model of in vitro plowing tests of the temporomandibular joint disc. Ann. Biomed. Eng. 37 (6), 1152–1164.

Srinivas, R., Sorsa, T., Tjäderhane, L., et al., 2001 May. Matrix metalloproteinases in mild and severe temporomandibular joint internal derangement synovial fluid. Oral Surg. Oral Med. Oral Pathol. Oral Radiol. Endod. 91 (5), 517–525.

Stolz, M., Raiteri, R., Daniels, A.U., VanLandingham, M.R., Baschong, W., Aebi, U., 2004 May May. Dynamic elastic modulus of porcine articular cartilage determined at two different levels of tissue organization by indentation-type atomic force microscopy. Biophys. J. 86 (5), 3269–3283.

Tanaka, E., Koolstra, J.H., 2008 Nov. Biomechanics of the temporomandibular joint. J. Dent. Res. 87 (11), 989–991.

Tanaka, E., van Eijden, T., 2003. Biomechanical behavior of the temporomandibular joint disc. Crit Rev Oral Biol Med. Crit Rev Oral Biol Med. 14 (2), 138–150.

Tanaka, E., Shibaguchi, T., Tanaka, M., Tanne, K., 2000 Sep. Viscoelastic properties of the human temporomandibular joint disc in patients with internal derangement. J. Oral Maxillofac. Surg. 58 (9), 997–1002.

Tanaka, E., Kikuzaki, M., Hanaoka, K., et al., 2003 Oct. Dynamic compressive properties of porcine temporomandibular joint disc. Eur. J. Oral Sci. 111 (5), 434–439.

Tanaka, E., Hirose, M., Yamano, E., et al., 2006 Feb. Age-associated changes in viscoelastic properties of the bovine temporomandibular joint disc. Eur. J. Oral Sci. 114 (1), 70–73.

Tanaka, E., Pelayo, F., Kim, N., Lamela, M.J., Kawai, N., Fernández-Canteli, A., 2014 May 7. Stress relaxation behaviors of articular cartilages in porcine temporomandibular joint. J. Biomech. 47 (7), 1582–1587.

Ventre, M., Mollica, F., Netti, P.A., 2009 Mar 11. The effect of composition and microstructure on the viscoelastic properties of dermis. J. Biomech. 42 (4), 430–435.

Vergroesen, P.-P.A., Kingma, I., Emanuel, K.S., et al., 2015 Jul. Mechanics and biology in intervertebral disc degeneration: a vicious circle. Osteoarthr. Cartil. 23 (7), 1057–1070.

Virca, G.D., Mallya, R.K., Pepys, M.B., Schnebli, H.P., 1984. Quantitation of human leukocyte elastase, cathepsin G, α-2-macro-globulin and α-1-proteinase inhibitor in osteoarthrosis and rheumatoid arthritis synovial fluids. Adv. Exp. Med. Biol. 167, 345–353.

Weisbecker, H., Viertler, C., Pierce, D.M., Holzapfel, G.A., 2013 Jul 26. The role of elastin and collagen in the softening behavior of the human thoracic aortic media. J. Biomech. 46 (11), 1859–1865.

Werner, J.A., Tillmann, B., Schleicher, A., 1991. Functional anatomy of the temporomandibular joint. A morphologic study on human autopsy material. Anat. Embryol. 183 (1), 89–95.

Willard, V.P., Kalpakci, K.N., Reimer, A.J., Athanasiou, K.A., 2012 Jan. The regional contribution of glycosaminoglycans to temporomandibular joint disc compressive properties. J. Biomech. Eng. 134 (1), 011011.

Wong, M., Ponticiello, M., Kovanen, V., Jurvelin, J.S., 2000 Sep. Volumetric changes of articular cartilage during stress relaxation in unconfined compression. J. Biomech. 33 (9), 1049–1054.

Yapp, C., Chen, Q., 2015 Oct. The mechanical, structural, and compositional changes of tendon exposed to elastase. Ann. Biomed. Eng. 43 (10), 2477–2486.

Yuan, H., Kononov, S., Cavalcante, F.S., Lutchen, K.R., Ingenito, E.P., Suki, B., 1985. Effects of collagenase and elastase on the mechanical properties of lung tissue strips. J. Appl. Physiol. 89 (1), 3–14 2000 Jul.

Zernia, G., Huster, D., 2006 Dec. Collagen dynamics in articular cartilage under osmotic pressure. NMR Biomed. 19 (8), 1010–1019.